nature photonics

LETTERS

PUBLISHED ONLINE: 21 MARCH 2010 | DOI: 10.1038/NPHOTON.2010.33

Soliton–similariton fibre laser

Bulent Oktem[1], Coşkun Ülgüdür[2] and F. Ömer Ilday[2]*

Rapid progress in passively mode-locked fibre lasers[1–6] is currently driven by the recent discovery of new mode-locking mechanisms, namely, the self-similarly evolving pulse (similariton)[7] and the all-normal-dispersion (dissipative soliton) regimes[8,9]. These are fundamentally different from the previously known soliton[10] and dispersion-managed soliton (stretched-pulse)[11] regimes. Here, we report a fibre laser in which the mode-locked pulse evolves as a similariton in the gain segment and transforms into a regular soliton in the rest of the cavity. To our knowledge, this is the first observation of similaritons in the presence of gain, that is, amplifier similaritons, within a laser cavity. The existence of solutions in a dissipative nonlinear cavity comprising a periodic combination of two distinct nonlinear waves is novel and likely to be applicable to various other nonlinear systems. For very large filter bandwidths, our laser approaches the working regime of dispersion-managed soliton lasers; for very small anomalous-dispersion segment lengths it approaches dissipative soliton lasers.

Passively mode-locked fibre lasers are being used in a diverse range of applications, including optical frequency metrology[12,13], material processing[14] and terahertz generation[15]. Historically, major advances in laser performance have followed the discovery of new mode-locking regimes[1–6,16], so there is always a strong motivation to search for new regimes.

The physics of mode-locked fibre lasers comprises a complex interaction of gain, dispersion and nonlinear effects[17]. Such lasers are a convenient experimental platform for the study of nonlinear waves subject to periodic boundary conditions and dissipative effects. These characteristics profoundly alter the behaviour of nonlinear waves, so this area of research is interesting in its own right. In addition to the vast literature on optical solitons[18], optical similaritons have recently emerged as a new class of nonlinear waves[19]. Other researchers[20–23] have demonstrated their existence in fibre amplifiers. These results have extended earlier predictions of parabolic pulse propagation in passive fibres by Anderson and colleagues[24] and experiments on amplification at normal dispersion[25]. Similaritons were first observed in a laser cavity by Ilday and colleagues[7]. These similaritons existed in segments of the cavity without any gain and loss to avoid the large spectral broadening that is characteristic of amplifier similaritons. Formation of a self-consistent solution in a laser cavity requires the compensation of spectral broadening, which has proved to be non-trivial[5]. Despite numerical predictions of their existence dating back almost a decade[26], amplifier similaritons had yet to be observed in a laser cavity.

Here, we present our experimental and theoretical work demonstrating an entirely new mode-locking regime, in which the pulse propagates self-similarly in the gain fibre with normal dispersion, and following spectral filtering, gradually evolves into a soliton in the rest of the cavity, where the dispersion is anomalous. All mode-locked lasers to date have had a single type of nonlinear wave propagating within the cavity; however, in our laser, distinctly different similariton and soliton pulses co-exist, demonstrating that transitions between these are possible. Remarkably, this construct is extremely robust against perturbations. Although the pulse experiences nonlinear effects strong enough to cause unprecedented, order-of-magnitude variations of the spectral bandwidth, the laser shows excellent short- and long-term stability.

A schematic model for the laser is illustrated in Fig. 1a. Numerical simulations of the model laser, based on a modified nonlinear Schrödinger equation, are used to analyse its operation. Parameters are chosen to match the experimental values. (Further details can be found in the Methods.) The solution obtained for a filter bandwidth of 15 nm and net group velocity dispersion (GVD) of $\beta_{\mathrm{net}}^{(2)} = 0.0136\ \mathrm{ps}^2$ illustrates the principle characteristics of the laser operation. The evolution is illustrated by plots of the pulse duration and spectral bandwidth as functions of position in the cavity (Fig. 1a). The gain fibre has normal GVD, where the incident pulse evolves into an amplifier similariton. A bandpass filter then filters the spectrum. Following the filter, the pulse enters a long segment of single-mode fibre (SMF) with anomalous GVD, and it evolves into a soliton in the long SMF segment. Because the pulse energy can easily exceed that of a fundamental soliton by up to a factor of 2, it undergoes soliton compression before its temporal and spectral widths stabilize. Similaritons have parabolic temporal profiles with linear chirp, and their temporal as well as spectral widths grow exponentially. In contrast, the first-order soliton pulse has a hyperbolic secant temporal profile and maintains a constant shape both in time and frequency, balancing nonlinear effects with dispersion. The transition from similariton to soliton is initiated by the bandpass filter, which filters both in the time and frequency domains due to the large chirp present. When the soliton re-enters the gain medium, it is shaped back into a similariton, which is an attractor state for any input pulse shape[22]. A closer look confirms that a parabolic temporal profile with linear frequency chirp is obtained at the end of the gain fibre and a chirp-free hyperbolic secant profile is obtained at the end of the SMF (Fig. 2).

Guided by the simulation results, we constructed an erbium-doped fibre laser (Fig. 3). Characterization results for the laser operating with a 12-nm-wide filter and $\beta_{\mathrm{net}}^{(2)} = 0.0136\ \mathrm{ps}^2$ are shown in Fig. 4. We measured full-width at half-maximum (FWHM) values of 12, 64 and 85 nm for the optical spectra from the 1%, 5% and polarization rejection ports, respectively (Fig. 4a,b). The corresponding spectral broadening ratio was 7.1. Figure 4a,b shows a good match between the simulations and the experiments. Pulse shapes were inferred from autocorrelation and spectrum measurements using the PICASO algorithm[27,28]. The pulse shapes agree well with numerical simulations and match a parabolic (hyperbolic secant) temporal profile for the similariton (soliton-like) pulses shortly after the end of the gain fibre (near the end of the SMF section; Fig. 4c,d). The laser generates ~750-fs-long chirped pulses from the nonlinear polarization evolution (NPE) port, which are compressed to 110 fs with a 1.2-m-long ($-0.03\ \mathrm{ps}^2$ of dispersion) SMF fibre outside the laser cavity. A zero-phase Fourier-transform calculation yields a theoretical lower limit of 75 fs, as

[1]Graduate Program of Materials Science and Nanotechnology, Bilkent University, 06800, Ankara, Turkey, [2]Department of Physics, Bilkent University, 06800, Ankara, Turkey. *e-mail: ilday@bilkent.edu.tr

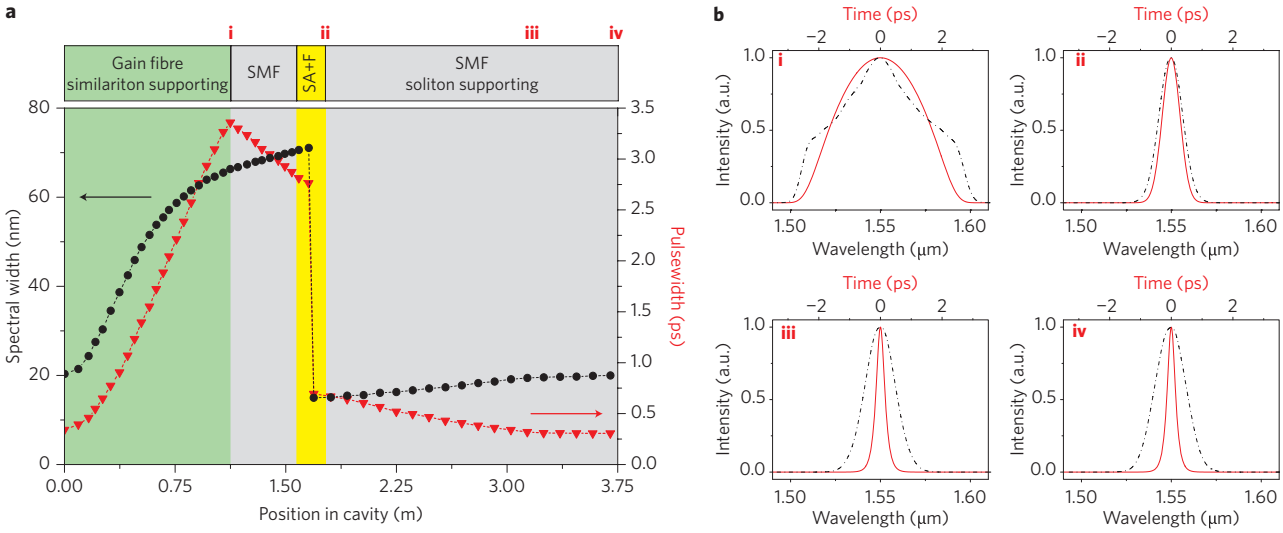

Figure 1 | Pulse evolution in the laser. a, Conceptual model of the laser with snapshots of different sections: at the end of the gain fibre (i), after the filter (ii), inside the SMF (iii), at the entrance of the gain fibre (iv). SA + F denotes the saturable absorber and the optical bandpass filter. Evolution of the spectral width (FWHM, black circles) and the pulsewidth (FWHM, red triangles) is plotted along the cavity. The shaded regions correspond to the main sections of the conceptual model. **b**, Snapshots of the temporal (red, solid lines) and spectral (black, dash-dotted lines) profiles of the pulse at the indicated locations.

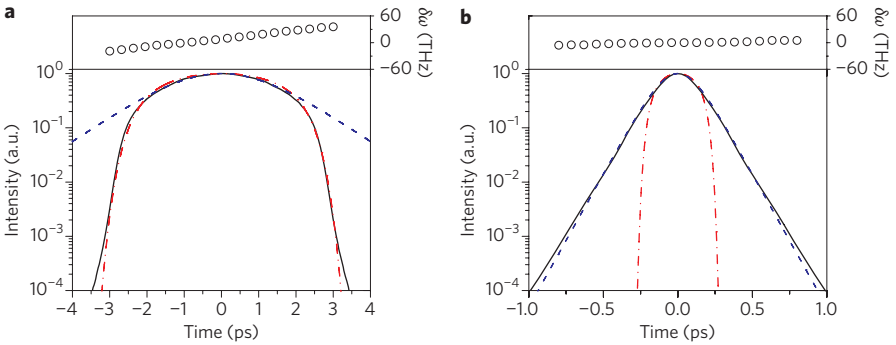

Figure 2 | Numerical simulation results. a,**b**, Temporal intensity and chirp profiles obtained at the end of the gain fibre (**a**) and the SMF (**b**). Black solid curve, intensity profile obtained through simulation; curve formed from black open circles, chirp profile; blue dashed curve, sech^2 fit, red dash–dotted curve, parabolic fit.

shown in inset of Fig. 4f. The uncompressed FWHM widths of the pulses from the 5% and 1% ports are 0.82 ps (assuming parabolic shape) and 0.28 ps (assuming $\mathrm{sech}^2(t)$ shape), respectively (Fig. 4e,f). The laser is very stable both in the short and long term. The RF spectrum shows 105 dB (>120 dB, limited by the measurement) suppression of noise, including (excluding) the side-bands at 50 and 100 Hz coupled from the power supply (inset of Fig. 4e). Also, the laser maintains uninterrupted mode-locked operation for many weeks.

To gain a broader understanding of the mode-locking dynamics, we investigated the effect of net dispersion and filter bandwidth on the spectral breathing ratio. To investigate the effect of varying dispersion, the filter bandwidth was set at 12 nm and the net dispersion was varied as shown in Fig. 5a. Simulations and experiments indicate that a small positive dispersion of 0.013 ps^2 maximizes the spectral breathing. The behaviour of the laser at the large anomalous GVD limit follows the soliton-like regime, the pulses being significantly narrower in bandwidth and, correspondingly, the effect of the filter being weakened[29]. In the case of large normal dispersion, the limiting behaviour is that of the all-normal dispersion fibre laser[8]. The maximum bandwidth is ultimately limited by the gain, and the filter dictates the lower limit to the bandwidth. Decreasing the filter bandwidth increases the breathing

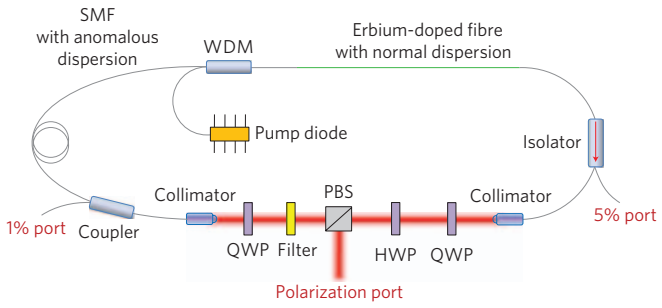

Figure 3 | Experimental set-up. Simplified schematic of the erbium-doped fibre laser. QWP, quarter wave plate; HWP, half wave plate; PBS, polarizing beamsplitter; WDM, wavelength-division multiplexer; SMF, single-mode fibre.

ratio up to a maximum of ~9 for a filter bandwidth of 8 nm at $\beta_{\mathrm{net}}^{(2)} = 0.0136\ \mathrm{ps}^2$ (Fig. 5b). A further decrease of the bandwidth increases the cavity losses and the regeneration of the spectrum becomes increasingly difficult. Mode-locking is unattainable for filter bandwidths lower than 3 nm. We numerically explored increasing the pulse energy, the lengths of the gain fibre and SMF

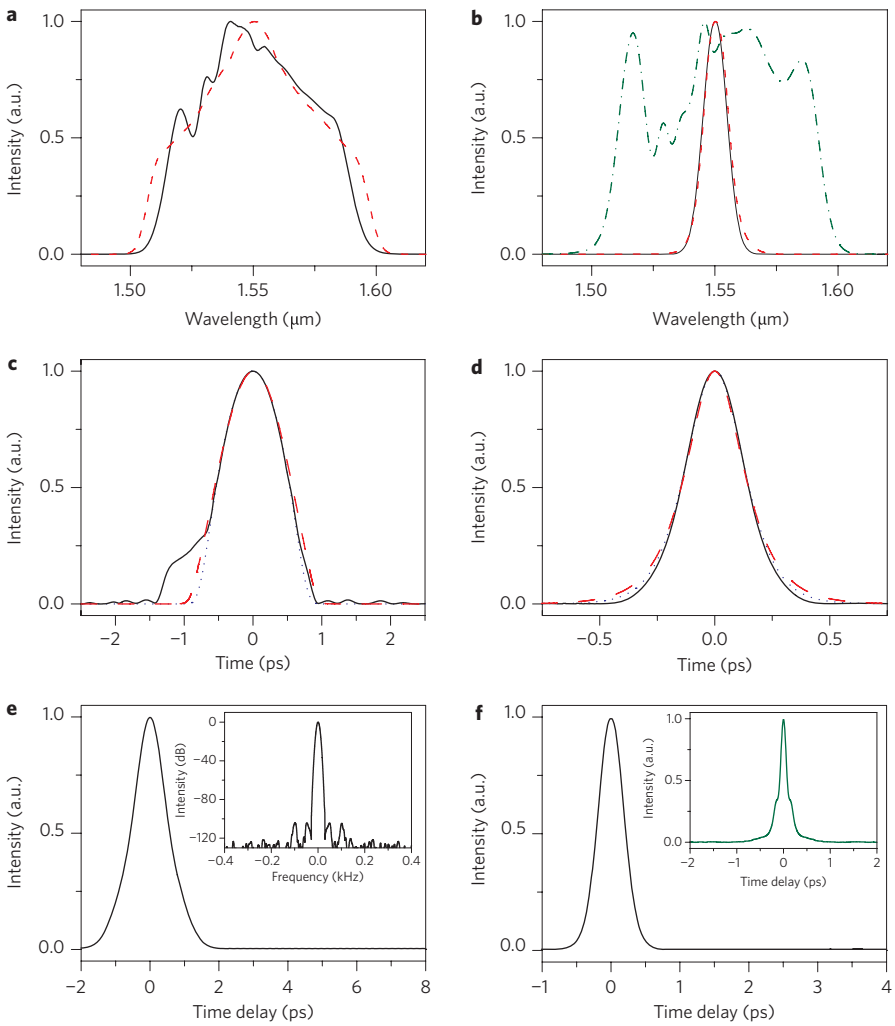

Figure 4 | Comparison of experimental and numerical results for operation at $\beta_{net}^{(2)} = 0.0136$ ps^2. **a**,**b**, Measured (black solid curve) and corresponding numerically simulated (red dashed curve) spectra of the pulse from the 5% port (**a**) and the 1% port (**b**). The measured spectrum (green dash-dotted curve, **b**) of the pulse from the NPE rejection port is also plotted to show the spectral breathing. **c**,**d**, PICASO retrieved (black solid curve) and numerically simulated temporal intensity profile (red dashed curve) of the pulse from the 5% port with a parabolic fit (blue dotted curve) (**c**) and from the 1% port with a sech^2 fit (blue dotted curve) (**d**). **e**,**f**, Intensity autocorrelation of the pulse from the 5% port (**e**), the 1% port (**f**) and NPE rejection port (**f**, inset), and the RF spectrum of the repetition of the laser with the central frequency shifted to zero for clarity (**e**, inset).

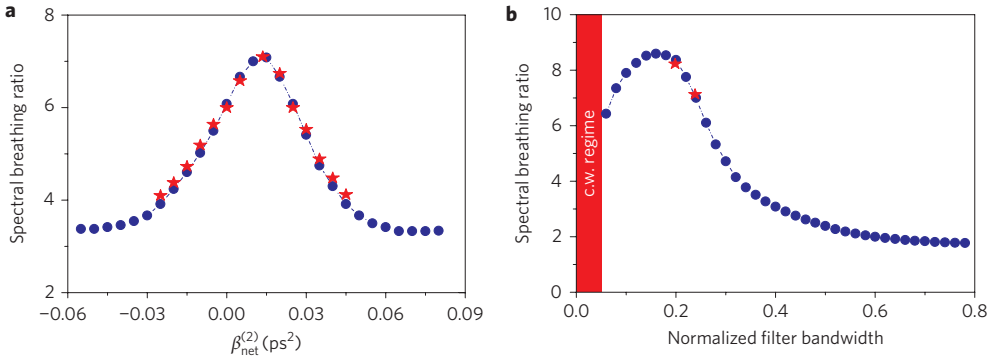

Figure 5 | Spectral breathing ratio of the laser. **a**, Dependence on the net GVD of the laser cavity: the red stars (blue spheres) show the experimental (numerical) results. **b**, Dependence on filter bandwidth normalized to the gain bandwidth of 50 nm: the red stars indicate the experimental result at 10 and 12 nm filter bandwidth and the blue spheres represent the numerical results.

for different values of the filter bandwidth and net dispersion to determine the maximum spectral breathing ratio. We obtained spectral breathing as much as 13 times greater for a 7-nm-wide filter, also at $\beta_{net}^{(2)} = 0.013$ ps^2.

In conclusion, we report a novel mode-locking regime of an erbium-doped fibre laser, with similariton and soliton propagation occurring in each half of the cavity. The similaritons are of the amplifier type, which constitutes their first experimental

observation inside a laser cavity. Indeed, we can interpret this mode of operation as a dissipative similariton, where the dissipation is viewed in a general sense of energy non-conservation and not necessarily only loss; in this way we may anticipate further links of this work with the wider class of nonlinear dynamics in non-Hamiltonian systems. The combination of an optical filter to undo the spectral broadening of the amplifier similariton and soliton formation to reshape the pulse into a chirp-free pulse, which can reseed the similariton formation, is the key step in overcoming the instabilities that have prevented the experimental demonstration of an amplifier similariton laser for nearly a decade[5,26]. The transitions between the similariton and soliton-like pulses are inherently interesting due to their vastly different characteristics and lead to variations of the spectral width of the pulse by an order of magnitude, an unprecedented factor. In the limit of increasing filter bandwidth, the laser becomes identical to the dispersion-managed soliton laser. In the other extreme of vanishing SMF section, the cavity becomes identical to that of an all-normal-dispersion laser. Thus, this new mode-locking regime sits at a nexus of all other known regimes of operation. Finally, it is remarkable that, in spite of the influence of these strong nonlinear effects, the laser is easier to mode-lock and more robust than any erbium-fibre laser incorporating NPE in our experience. The asymptotic attractive nature of the amplifier similariton may be key to the increased robustness against perturbations and low-noise operation of the laser (see Supplementary Information for the noise characterization of the laser).

Methods

Numerical simulations are based on a modified nonlinear Schrödinger equation:

$$\frac{\partial U}{\partial z} + i\frac{\beta^{(2)}}{2}\frac{\partial^2 U}{\partial \tau^2} - \frac{\beta^{(3)}}{6}\frac{\partial^3 U}{\partial \tau^3} = \frac{g}{2}U + i\gamma|U|^2 U + i\gamma T_R \frac{\partial |U|^2}{\partial \tau}U$$

Here, $U = U(z, \tau)$ is the slowly varying amplitude of the pulse envelope, z the propagation coordinate, and τ the time delay parameter. $\beta^{(2)}$ and $\beta^{(3)}$ are the second-order (GVD) and third-order dispersion (TOD) parameters, respectively. γ is the nonlinearity parameter given by $\gamma = n_2\omega_0/cA_{\mathrm{eff}}$, where n_2 is the Kerr coefficient, ω_0 the central angular frequency, c the velocity of light in vacuum, and A_{eff} the effective mode area. $T_R = 5$ fs is related to the slope of the Raman gain spectrum, which is assumed to vary linearly with frequency around the central frequency. The gain is given by

$$g = \frac{g_{SS}}{1 + W/W_0 + (\omega - \omega_0)^2/\Delta\omega^2},$$

where $g_{SS} \approx 3.45$ is the small-signal gain (corresponding to 30 dB in power and non-zero only for the gain fibre), $\Delta\omega$ the gain bandwidth, which is chosen to correspond to 50 nm, and $W(z) = \int |U|^2 \, \mathrm{d}\tau$ is the pulse energy. The gain is assumed to saturate over a large number of pulses with a response time much longer than the cavity roundtrip time. As such, the saturated values of the gain along the erbium fibre are assumed to depend on average power only. W_0 is an effective gain saturation energy corresponding to the saturation power (determined by pump power) for a given repetition rate. The saturable absorber is modelled by a transfer function that describes its transmittance

$$T(\tau) = 1 - \frac{q_0}{1 + P(\tau)/P_0},$$

where q_0 is the unsaturated loss, $P(z, \tau) = |U(z, \tau)|^2$ the instantaneous pulse power, and P_0 the saturation power. The specific shape of the transmittance function is found not to be important. The numerical model is solved with a standard symmetric split-step beam propagation algorithm, and the initial field is white noise. The same stable solutions are reached from different initial noise fields.

The parameters used in the numerical simulations are the same as their experimental values. Experimentally, we are able to vary the net dispersion of the cavity (by varying the length of the SMF section), the pulse energy and use filters with bandwidth of either 10 or 12 nm, both of which are centred at 1,550 nm. The erbium-doped gain fibre is 1 m long, with a mode field diameter (MFD) of 3.57 μm, numerical aperture (NA) of 0.32, $\beta^{(2)} = 76.9$ fs^2 mm^{-1}, $\beta^{(3)} = 168$ fs^3 mm^{-1}, and $\gamma = 0.00932$ W^{-1} m^{-1} at 1,550 nm. The rest of the cavity comprises ~3 m (varied to adjust the net dispersion value) of SMF-28 just before the gain fibre and a total of 65 cm of OFS-980 as the lead fibres of the fibre components. SMF-28 has an MFD of 10.4 μm, NA of 0.14, $\gamma = 0.0011$ W^{-1} m^{-1}, $\beta^{(2)} = -22.8$ fs^2 mm^{-1} and $\beta^{(3)} = 86$ fs^3 mm^{-1}. The OFS-980 has an MFD of 7.5 μm, NA of 0.16, $\gamma = 0.0021$ W^{-1} m^{-1}, $\beta^{(2)} = 4.5$ fs^2 mm^{-1} and $\beta^{(3)} = 109$ fs^3 mm^{-1}. We set $P_0 = 2.13$ kW and $W_0 = 2.21$ nJ to obtain an intracavity pulse energy of 3.13 nJ, which is the measured value for a 12-nm-wide filter, $\beta^{(2)}_{\mathrm{net}} = 0.0136$ ps^2, and repetition rate of 39 MHz. For the results presented in Fig. 1 and Fig. 2, $\beta^{(2)}_{\mathrm{net}} = 0.0136$ ps^2 and the filter bandwidth is 15 nm. For the results presented in Fig. 4, $\beta^{(2)}_{\mathrm{net}} = 0.0136$ ps^2 and the filter bandwidth is 12 nm.

Experimentally, a maximum of 350 mW of pump light at 980 nm from a laser diode is delivered to the cavity by means of a 980/1,550 nm wavelength division multiplexer. Although continuous-wave (c.w.) output power can be as high as 150 mW, the intracavity power is limited to ~120 mW in mode-locked operation. An optical isolator ensures unidirectional operation. NPE, implemented with wave plates and a polarizer, functions as an artificial saturable absorber[30]. Self-starting mode-locked operation is achieved readily and very stably by adjustment of the wave plates. The repetition rate of the laser varies between 29 MHz (at $\beta^{(2)}_{\mathrm{net}} = -0.025$ ps^2) and 58 MHz (at $\beta^{(2)}_{\mathrm{net}} = +0.045$ ps^2). The pulse energy is limited to ~3.1 nJ, limited by the self-similar evolution in the gain fibre, which has a value of γ about a factor of 9 larger than that of regular fibre at 1,550 nm. At higher pulse energies, gain filtering starts to suppress further spectral broadening, which distorts self-similar propagation. It is easier to avoid overdriving the soliton propagation at higher energies because the output-coupling ratio can be increased. With the use of a suitably designed gain fibre, pulse energies exceeding 30 nJ should be possible.

We measure the intensity noise to be 0.008% (from 1 to 250 kHz) and timing jitter to be 27 fs (from 1 kHz to the Nyquist limit), even though no effort was made to improve the noise performance. These measurements suggest that this mode-locking regime may lead to lower relative intensity noise and phase noise compared to conventional fibre lasers.

Received 11 August 2009; accepted 8 February 2010; published online 21 March 2010

References

1. Buckley, J. R., Wise, F. W., Ilday, F. Ö. & Sosnowski, T. Femtosecond fiber lasers with pulse energies above 10 nJ. *Opt. Lett.* **30,** 1888–1890 (2005).
2. Kieu, K., Renninger, W. H., Chong, A. & Wise, F. W. Sub-100 fs pulses at watt-level powers from a dissipative-soliton fiber laser. *Opt. Lett.* **34,** 593–595 (2009).
3. Ruehl, A., Hundertmark, H., Wandt, D., Fallnich, C. & Kracht, D. 0.7 W all-fiber erbium oscillator generating 64 fs wave breaking-free pulse. *Opt. Express* **13,** 6305–6309 (2005).
4. Ortaç, B. *et al.* High-energy femtosecond dispersion compensation free fiber laser. *Opt. Express* **15,** 10725–10732 (2007).
5. Wise, F. W., Chong, A. & Renninger, W. H. High-energy femtosecond fiber lasers based on pulse propagation at normal dispersion. *Laser Photon. Rev.* **2,** 58–73 (2008).
6. Ruehl, A., Wandt, D., Morgner, U. & Kracht, D. Normal dispersive ultrafast fiber oscillator. *IEEE J. Sel. Top. Quantum Electron.* **15,** 170–181 (2009).
7. Ilday, F. Ö., Buckley, J. R., Clark, W. G. & Wise, F. W. Self-similar evolution of parabolic pulses in a laser. *Phys. Rev. Lett.* **92,** 213902 (2004).
8. Chong, A., Buckley, J., Renninger, W. & Wise, F. All-normal-dispersion femtosecond fiber laser. *Opt. Express* **14,** 10095–10100 (2006).
9. Renninger, W. H., Chong, A. & Wise, F. W. Dissipative solitons in normal-dispersion fiber lasers. *Phys. Rev. A* **77,** 023814 (1991).
10. Duling III, I. N. Subpicosecond all-fibre erbium laser. *Electron. Lett.* **27,** 544–545 (1991)
11. Tamura, K., Ippen, E. P. & Haus, H. A. Pulse dynamics in stretched-pulse fiber lasers. *Appl. Phys. Lett.* **67,** 158–160 (1995).
12. Newbury, N. R. & Swann, W. C. Low-noise fiber-laser frequency combs (invited). *J. Opt. Soc. Am. B* **24,** 1756–1770 (2007).
13. Schibli, T. *et al.* Optical frequency comb with submillihertz linewidth and more than 10 W average power. *Nature Photon.* **2,** 355–359 (2008).
14. Shah, L., Fermann, M. E., Dawson, J. W. & Barty, C. P. J. Micromachining with a 50 W, 50 μJ, sub-picosecond fiber laser system. *Opt. Express* **14,** 12546–12551 (2006).
15. Hoffmann, M. C. *et al.* Fiber laser pumped high average power single-cycle terahertz pulse source. *Appl. Phys. Lett.* **93,** 141107 (2008).
16. Nelson, L. E., Fleischer, S. B., Lenz, G. & Ippen, E. P. Efficient frequency doubling of a femtosecond fiber laser. *Opt. Lett.* **21,** 1759–1761 (1996).
17. Haus, H. A. Mode-locking of lasers. *IEEE J. Sel. Top. Quantum Electron.* **6,** 1173–1185 (2000).
18. Kivshar, Y. & Agrawal, G. P. *Optical Solitons: from Fibers to Photonic Crystals* (Academic Press, 2003).
19. Dudley, J. M., Finot, C., Richardson, D. J. & Millot, G. Self-similarity in ultrafast nonlinear optics. *Nature Phys.* **3,** 597–603 (2007).
20. Kruglov, V. I., Peacock, A. C., Dudley, J. M. & Harvey, J. D. Self-similar propagation of high-power parabolic pulses in optical fiber amplifiers. *Opt. Lett.* **25,** 1753–1755 (2000).

21. Kruglov, V. I., Peacock, A. C., Harvey, J. D. & Dudley, J. M. Self-similar propagation of parabolic pulses in normal-dispersion fibre amplifiers. *J. Opt. Soc. Am. B* **19,** 461–469 (2002).
22. Kruglov, V. I. & Harvey, J. D. Asymptotically exact parabolic solutions of the generalized nonlinear Schrödinger equation with varying parameters. *J. Opt. Soc. Am. B* **23,** 2541–2550 (2006).
23. Fermann, M. E., Kruglov, V. I., Thomsen, B. C., Dudley, J. M. & Harvey, J. D. Self-similar propagation and amplification of parabolic pulses in optical fibers. *Phys. Rev. Lett.* **84,** 6010–6013 (2000).
24. Anderson, D., Desaix, M., Karlsson, M., Lisak, M. & Quiroga-Teixeiro, M. L. Wave-breaking-free pulses in nonlinear-optical fibers. *J. Opt. Soc. Am. B* **10,** 1185–1190 (1993).
25. Tamura, K. & Nakazawa, M. Pulse compression by nonlinear pulse evolution with reduced optical wave breaking in erbium-doped fiber amplifiers. *Opt. Lett.* **21,** 68–70 (1996).
26. Peacock, A. C. *et al.* Generation and interaction of parabolic pulses in high gain fiber amplifiers and oscillators. *Conf. Opt. Fiber Commun.* 2000, Technical Digest, Paper WP4-1.
27. Nicholson, J. W., Jasapara, J., Rudolph, W., Omenetto, F. G. & Taylor, A. J. Full-field characterization of femtosecond pulses by spectrum and cross-correlation measurements. *Opt. Lett.* **24,** 1774–1776 (1999).
28. Finot, C. & Millot, G. Synthesis of optical pulses by use of similaritons. *Opt. Express* **12,** 5104–5109 (2004).
29. Noske, D. U. & Taylor, J. R. Spectral and temporal stabilisation of a diode-pumped ytterbium-erbium fibre soliton laser. *Electron. Lett.* **29,** 2200–2202 (1993).
30. Hofer, M., Fermann, M. E., Harberl, F., Ober, M. H. & Schmidt, A. J. Mode locking with cross-phase and self-phase modulation. *Opt. Lett.* **16,** 502–504 (1991).

Acknowledgements

This work was supported by the Scientific and Technological Research Council of Turkey (TÜBİTAK) grant no. 106G089, Marie Curie International Research Grant (IRG) grant no. 046585, EU 7th Framework project UNAM-REGPOT grant no. 203953, Bilkent University Internal Research Funds, and the Distinguished Young Scientist award of the Turkish Academy of Sciences (TÜBA). The authors would like to thank O. Aytür for critical reading of the manuscript.

Author contributions

B.O. and C.Ü. conducted the experiments and analysed the data. B.O. performed the numerical simulations. F.Ö.I. and B.O. wrote the paper with contributions from C.Ü.

Additional information

The authors declare no competing financial interests. Supplementary information accompanies this paper at www.nature.com/naturephotonics. Reprints and permission information is available online at http://npg.nature.com/reprintsandpermissions/. Correspondence and requests for materials should be addressed to F.Ö.I.